

Saturated and Unsaturated Mechanical Properties of Typical Soils Distributed in Northeast Thailand

Yuji KOHGO*
Surendra Bahadur TAMRAKAR**
Hui Gang TANG**

* *Crop Production and Postharvest Technology Division,
Japan International Research Center for Agricultural Sciences (JIRCAS)
Tsukuba, Ibaraki, 305 Japan*

** *School of Civil Engineering, Asian Institute of Technology
Pathumthani Thailand*

Received September 4, 1998

ABSTRACT

We clarified the saturated and unsaturated mechanical properties of typical soils distributed in Northeast Thailand. We sampled a soil with a yellow color (Yellow soil) as a typical soil. The mechanical properties of the Yellow soil were investigated by using oedometer, pressure plate and triaxial test apparatuses. The results of oedometer tests showed that yield stress increased as suction increased, the slopes of $e - \log \sigma_v$ (e : void ratio, σ_v : vertical stress) curves in the elastoplastic region were affected by the suction, and this soil expressed a large amount of volume reductions due to soaking of water. The results of the pressure plate tests showed that the air entry value was about 10kPa, and the volume change behavior due to suction was elastic when the suction value exceeded about 30kPa. The results of triaxial compression tests revealed that by comparing the specimens with the same confining pressures but different suction values, the higher suction the greater deviator stresses of specimens, the shear strength also increased with increasing suctions, however, the suction influence became weaker as the confining pressure increased.

Additional Key words: collapsible soil, sandy soil, suction, unsaturated soil.

Introduction

Northeast Thailand occupies an area of about 168,800 square kilometers and it accounts for about one third of the total area of the country. It is bounded in the north and east on the Mekong River and in the south and west on the Phanom Dong Rak and Phetchabun Mountain Ranges. The general physiography of this region mostly consists of an undulating high plateau interspersed with low-lying hills and wide sloping valleys. The Phu Phan Mountain Range, which lies in the northeast portion of the plateau, divides the plateau into two basins; the Khorat and the Sakon Nakhon Basins¹⁴). The climate is semi-arid. In spite of that an annual rainfall is over 1000mm, the amount of evaporation is greater than that of rainfall in most seasons.

Agricultural production in Northeast Thailand has been remarkably inhibited due to the following two main reasons. The first is that sandy and silty soils with a low fertility cover the area extensively. The second is that the supply of water is not stable. For example, the long term mean value of yield of rice in paddy fields without irrigation facilities still remains about 1.5t/ha. The value is rather lower than that of the whole country, 2t/ha¹³). Due to these factors, the farmers' income in the area is the lowest in Thailand. The Government of Thailand suggests that agriculture should be actively promoted in Northeast Thailand.

The total irrigated area accounts for about 20% of the whole farmland in Thailand¹⁵). The irrigated area is mainly concentrated in the Central Plain. The ratio of irrigated area in the Central Plain to the whole area irrigated reaches about 60%. However, the ratio in Northeast Thailand is rather smaller. The main irrigation facilities in this area are isolated ponds. The ponds are mainly built by digging the ground. Most of these ponds, however, have a low function due to salinization of reservoir water, collapse and erosion of the slopes of ponds. To alleviate these shortcomings, it is necessary to clarify the mechanical properties of the soils on or with which the ponds are constructed.

In this paper, we will only discuss the soils distributed in the Khorat Basin and clarify the saturated and unsaturated mechanical properties of

the typical soils in order to obtain basic information for the construction of irrigation facilities, especially small ponds.

Schematic review of mechanical properties of typical soils distributed in northeast thailand

Before the main discussion, we have to define some stress variables; suction s , total mean stress σ_m , net mean stress p , effective mean stress p' , and deviator stress q , as follows:

$$s = u_a - u_w \quad (1)$$

$$\sigma_m = \frac{1}{3} (\sigma_1 + 2\sigma_3) \quad (2)$$

$$p = \sigma_m - u_a \quad (3)$$

$$p' = \frac{1}{3} (\sigma'_1 + 2\sigma'_3) \quad (4)$$

$$q = \sigma_1 - \sigma_3 \quad (5)$$

$$s^* = \langle s - s_e \rangle \quad (6)$$

where u_a is the pore air pressure, u_w the pore water pressure, σ_1 the total maximum principal stress, σ_3 the total minimum principal stress, σ'_1 the effective maximum principal stress, σ'_3 the effective minimum principal stress, s^* the effective suction, s_e the air entry suction and the brackets $\langle \rangle$ denote the operation $\langle z \rangle = z$ at $z > 0$ and $\langle z \rangle = 0$ at $z \leq 0$.

1) Surface soils in northeast thailand

The geological map of Northeast Thailand is shown in Fig. 1³). It found from this figure that the Khorat Basin was widely covered with sediments of sandstones and siltstones denoted by symbols k_{ms} or k_{kk} . The symbol Q denotes the Quaternary deposits.

Udomchoke¹⁴) summarized the surface soils in the Khorat Basin by referring to the Boonsaner's¹) and Chong's²) works. According to his work, the surface soils are classified into; (1) Residual soils of Khorat Group rocks, (2) Gravel beds, (3) Laterites, (4) Red and Yellow loessial soils, (5) Windblown sand deposits, (6) Old alluvium, (7) Alluvium, and (8) Lake and swamp deposit. It was pointed out that the following engineering problems; collapse due to wetting, erosion and dispersion, might exist in these soils. The possibilities of the problems for each soil are summarized in Table 1. Erosion and collapse due

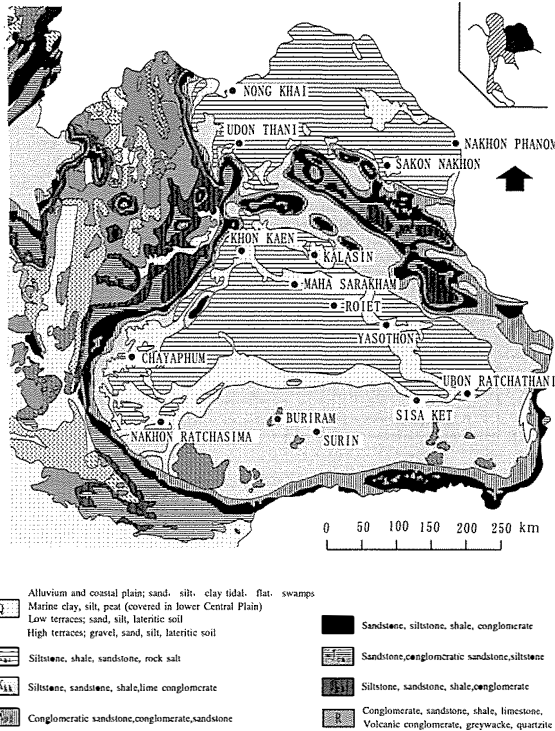


Fig.1. Geological map of Northland Thailand. ³⁾

to wetting may be problems for sandy soils while dispersion becomes a problem for some clayey soils. As described before, most of the soils distributed in Northeast Thailand are sandy soils. Then, the main problems are erosion and collapse due to wetting.

Some typical soil profiles and their locations are

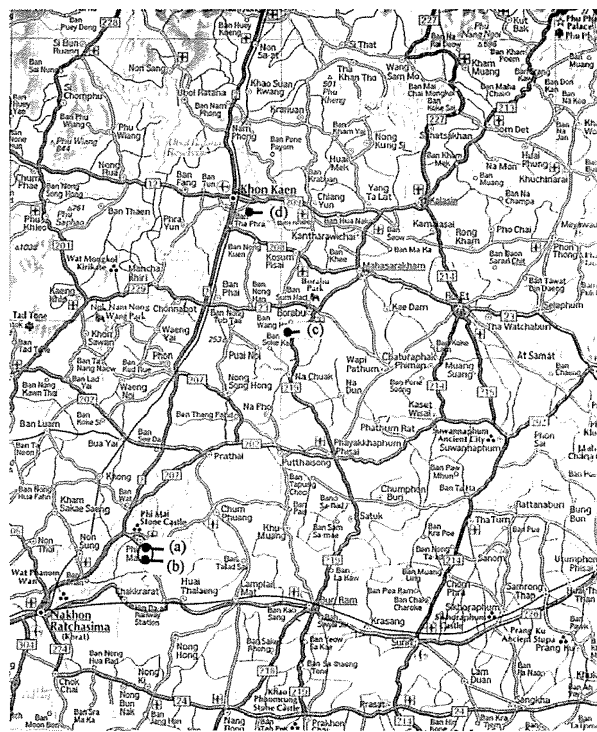


Fig.3 Location of typical soil profiles.

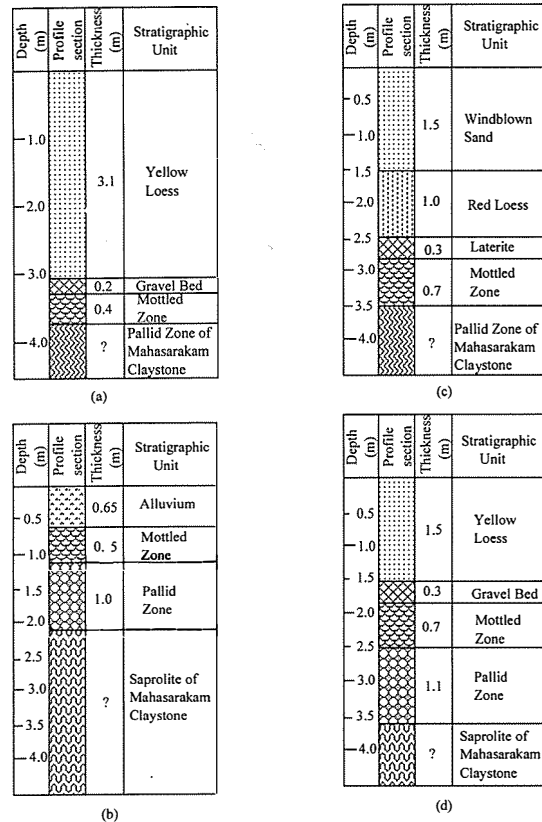


Fig.2. Typical soil profiles in Khorat Basin (Udomchoke, ¹⁴⁾).

shown in Figs. 2 and 3, respectively. Fig. 2 shows that residual soils, gravel beds or laterites, loesses and windblown sand orderly deposit from the bottom to the top.

2) Mechanical properties of typical soils

(1) Physical properties

The typical grading curves of some soils described above are shown in Fig. 4. Figs. 4 (a), (b), (c) and (d) show the grading curves for residual soils, loessial soils, windblown sand and old alluvial deposit, respectively. The gradation curves of residual soils strongly depend on their parent rocks. If the parent rock is sandstone, the content of sand exceeds 90%.

Table1. Summary of problematic of soils in Khorat Basin (data from Udomchoke ¹⁴⁾)

Soils	Collapse	Erosion	Dispersion
Residual soils			
Lowland	No	No	Yes
Highland	Yes	Yes	No
Red loess	Yes	Yes	No
Yellow loess	Yes	Yes	No
Windblown sand	Yes	Yes	No
Old alluvium	No	Yes	No
Alluvium	No	No	Yes
Lake and swamp deposits	No	No	No

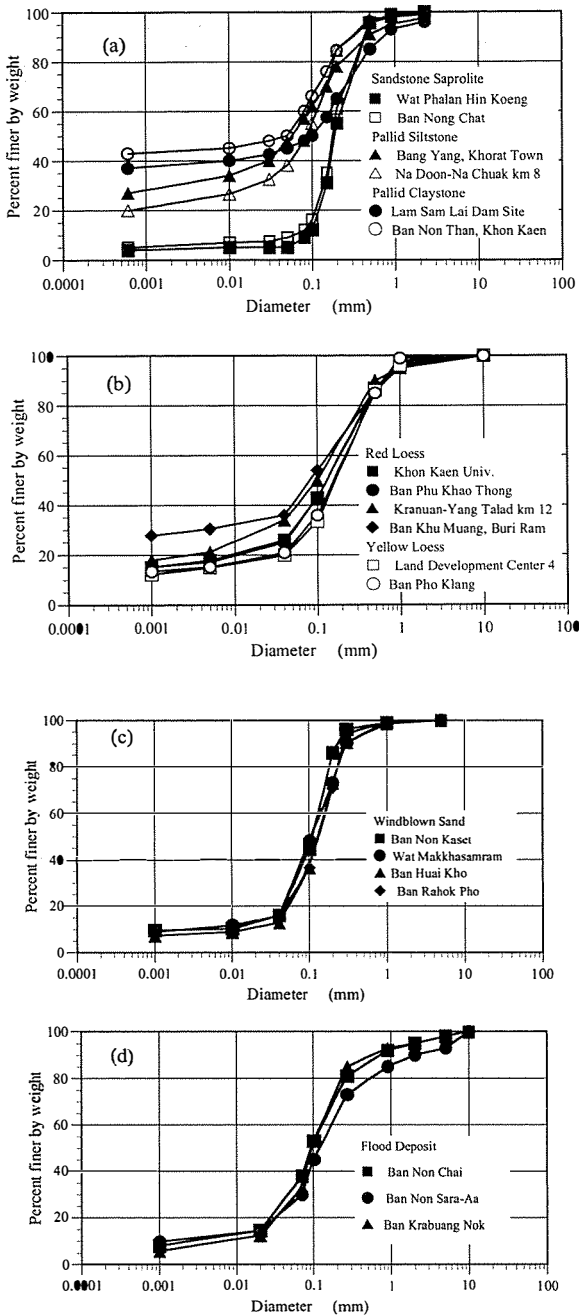


Fig.4. Grading curves of soil sample Khorat Basin. (data from Udomchoke ¹⁴)
 (a) Residual soil, (b) Loessial soils,
 (c) Windblown sand, (d) Old alluvial deposit.

If the parent rock is siltstone or claystone, the contents of sand, silt and clay are about 50%, 25% and 25%, respectively for siltstone and for claystone about 50%, 10% and 40%, respectively. In loessial soils, the contents of sand, silt and clay are 50~70%, about 20% and 10~30%, respectively. The windblown sand contains about 90% of fine sand and small amounts of silt and clay particles. The old

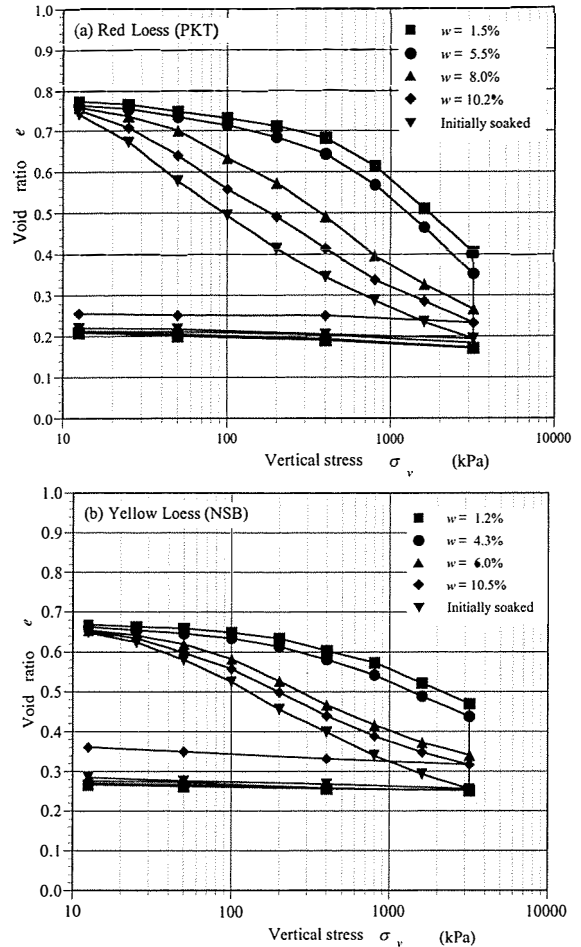


Fig.5. Oedometer test results undisturbed Red and Yellow Loesses (data from Udomchoke ¹⁴).

alluvium deposit is composed of 80-90% of sand and 10-20% of silt and clay. The alluvial deposit has 50~80% of sand and 50-20% of silt and clay. In lake and swamp deposit, the contents of sand, silt and clay are about 50%, about 10% and about 40%, respectively. One of the common characteristics to all the soils is that they contain a large amount of fine sands.

(2) Mechanical properties

The mechanical properties of the Red and Yellow Loesses were also investigated. Fig. 5 shows the results of oedometer tests for undisturbed Red and Yellow Loesses with various initial water contents. From these results, it found that the specimens with lower initial water contents had larger yield stresses. This feature is one of the typical properties of unsaturated soils.

Fig. 6 shows the soil-water retention curves for the Red and Yellow Loesses sampled from various sites. The air entry values of both soils are within the

suction range $s_e = 5\sim 10\text{kPa}$. According to our classification of unsaturated conditions¹⁰⁾, the suction ranges for Yellow Loesses correspond approximately to insular air saturation; $s \leq 5\sim 10\text{kPa}$, fuzzy saturation; $5\sim 10\text{kPa} \leq s < 200\text{kPa}$, and pendular saturation conditions; $s \leq 200\text{kPa}$, respectively. For Red Loess, they are approximately insular air saturation; $s \leq 5\sim 10\text{kPa}$, fuzzy saturation; $5\sim 10\text{kPa} \leq s < 100\text{kPa}$, and pendular saturation conditions; $s \geq 100\text{kPa}$, respectively.

Fig. 7 shows the triaxial compression test (CD test) results for Yellow Loess. The CD tests were conducted for saturated specimens. The stress-strain curves express the strain-hardening behavior and are consistent with those of typical loose sands. The

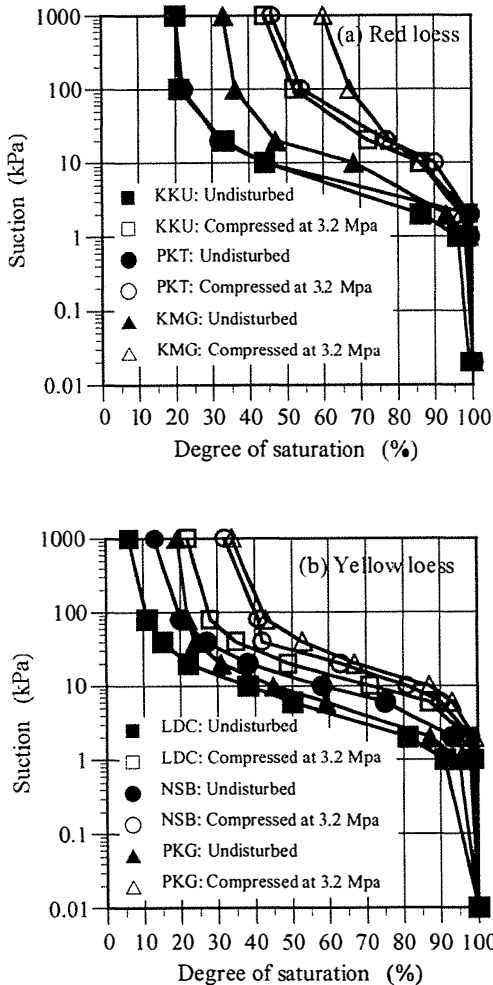


Fig.6. Soil water retention curves (a) Red loesses (b) Yellow loesses (data from Udomchoke¹⁴⁾).
 KKU: Khon Kaen University LDC: Land Dev. Dept. Center
 PKT: Ban Phu Khao Thong
 NSB: Ban Non Som Boom, Khon Kaen
 KMG: Ban Khu Muang, PKG: Ban Pho Klamg

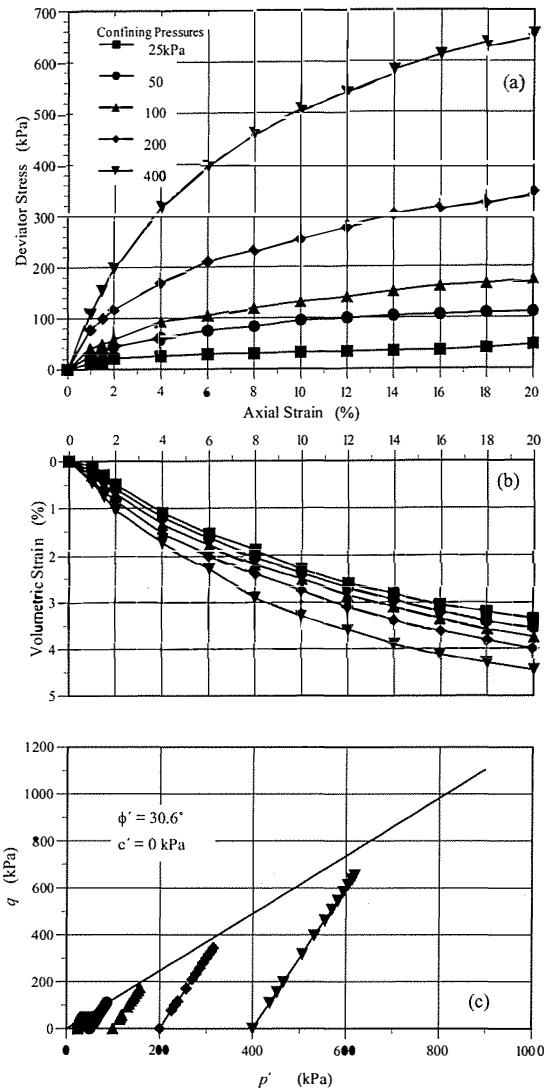


Fig.7. Triaxial compression test (CD test) results for Yellow Loess, (a) Stress-strain relationships, (b) Volumetric strain-axial strain relationships, (c) Stress paths during shear.¹⁴⁾

volume change is of compressive behavior and is similar to that of typical loose sands. The internal friction angle of the Yellow Loesses is about 30 degrees.

Mechanical properties of typical soils sampled from Khao Suan Kwang near Khon Kaen City

In the previous section, we reviewed the typical mechanical properties of the soils distributed in Northeast Thailand. In this section, we will mainly describe in more detail saturated and unsaturated properties of a soil with a yellow color, which may be associated to Yellow Loess.

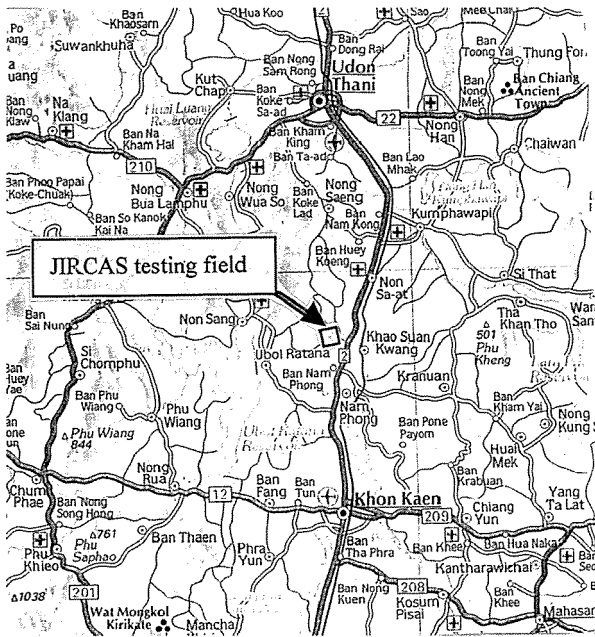


Fig. 8. Schematical location of JIRCAS testing field.

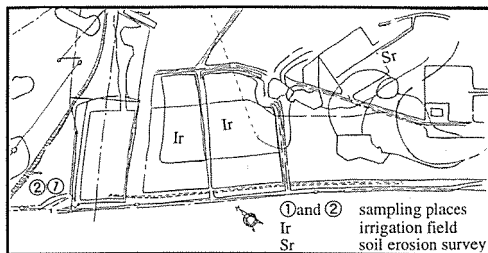


Fig. 9. JIRCAS testing field in Khao Suan Kwang and sampling places.

1) Soil samples and experimental test procedures

Two kinds of soils sampled at the JIRCAS testing field in Khao Suan Kwang near Khon Kaen City in June 1996 were used in this study. The location of the JIRCAS testing field is shown in Fig. 8. These soils were designated as Gray and Yellow soils after their color. Sampling places are denoted as points ① and ② in Fig. 9. The soils sampled from the points ① and ② are respectively Gray and Yellow soils. We conducted some in-situ and laboratory tests. They are field density, physical property, compaction, oedometer, plate pressure and triaxial compression tests. For the Yellow soil, all the tests were carried out while only field density tests, physical property tests and compaction tests were conducted for the Gray soil. Here, we will only describe the procedures of the tests conducted to investigate the properties of the unsaturated Yellow soil, namely oedometer, pressure plate and triaxial compression tests.

(1) Preparation of soil samples

From previously uniformly mixed soil batches, the required amount of soil was oven-dried at the temperature of 105 °C for at least 24 hours. After oven drying, the soils were kept in a desiccator until they cooled down. Then the packets of soil particles were crushed with a rubber hammer. Particles were then stored in plastic bags.

At least before one week of testing, a required amount of the dried soil was taken out from a bag and once again oven-dried for 24 hours. After cooling down, a required amount of distilled water was added to the oven-dried soil with a sprayer. After sufficient mixing, the soil was put into a plastic bag and the bag was sealed. It was kept for more than 24 hours.

(2) Oedometer test

In order to investigate the volume change behavior of the unsaturated Yellow soil due to external loads, oedometer tests with and without soaking of water were conducted. The oedometer was of a standard type and consisted of a confining ring, top cap with a coarse porous stone, base plate with a coarse porous stone and a water reservoir pan. As in this study, specimens were unsaturated, the sponges which were previously submerged and then put into open packages made of plastic bags covered the specimens to prevent vaporization

The samples were compacted so that the initial dry density was consistent with the field dry density (1.2g/cm^3) under initial water contents of 2, 4, 6, 8, 12 and 30%. However, as the specimens with initial water content of 30% could not exhibit the initial dry density, they were compacted as loosely as possible. The dimensions of the specimens are 63.5mm in diameter and 19.0mm in height. The other testing procedure followed the recommendations of JFS T 411-1990⁶⁾.

(3) Pressure plate test

In order to investigate the volume change behavior of the unsaturated Yellow soil due to suction, pressure plate tests were conducted. The pressure plate apparatus produced by Soil Moisture Equipment Co. Ltd. was used. The apparatus consists of a pressure chamber, a ceramic plate with a high air entry value (more than 1,500kPa), and air pressure and negative pore water pressure applying

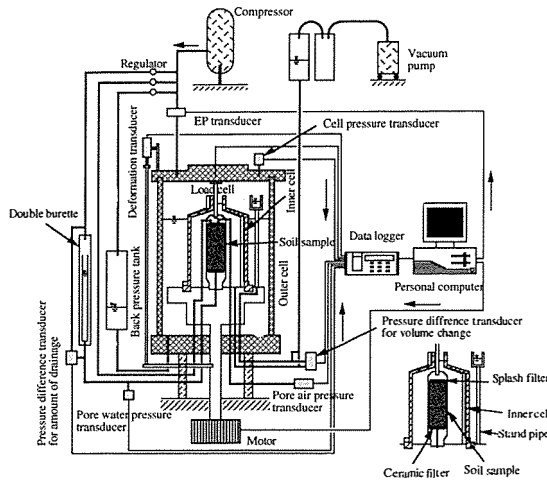


Fig.10. Triaxial compression test apparatus for unsaturated soils.

systems. The negative pore water pressure applying system is used to apply specimens suction under $u_a = 0\text{kPa}$ when the suction is lower than 10kPa (about 100cm H₂O head), while the air pressure applying system is used under $u_w = 0\text{kPa}$ when the suction is higher than 10kPa.

The specimens were prepared by carefully packing the slurry sample, with about 1.5 times the water content of the liquid limit, into retaining rings to avoid air trapping into specimens. The dimensions of the specimens are about 50mm in diameter and 10mm in height.

Two series of tests were conducted. Series I consisted of only the suction increasing process (drying) and series II included suction increasing and decreasing processes (drying and wetting). In each test, the specimens were taken out one by one from the chamber to measure the water content and the dimension of the specimen under each suction equilibrium condition. Therefore, 10 or 13 specimens were used in each test.

(4) Triaxial compression test

The triaxial compression test apparatus used in this study was specially designed for investigating the mechanical properties of unsaturated soils. The apparatus is shown in Fig. 10. The advantages of the apparatus are that pore air and pore water pressures can be separately applied to soil specimens, that the double cell structure is employed in order to measure accurately the volume changes, and that the test data can be measured automatically.

The Yellow soil was statically compacted by using a piston rod so that the specimens had the initial dry density 1.2g/cm³ and the initial water content 8%. The initial conditions were consistent with the field conditions. The height and diameter of the sample were 10cm and 5cm, respectively.

Axis translation technique⁵⁾ was adopted here. At first the specimens were consolidated due to suctions and then consolidated due to confining pressures. The shear tests were carried out under constant suction conditions. The suction values applied were 0, 50, 100 and 200kPa, and the confining pressures applied were 50, 150 and 200kPa.

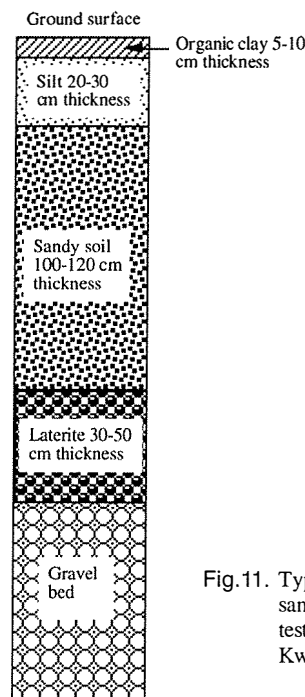


Fig.11. Typical soil profile at the sampling sites, JIRCAS testing field in Khao Suan Kwang, Northeast Thailand.

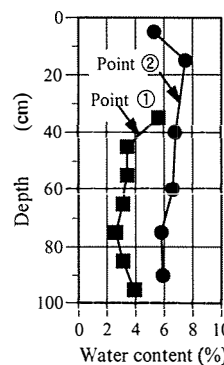


Fig.12. Changes of water content with depth at sampling sites.

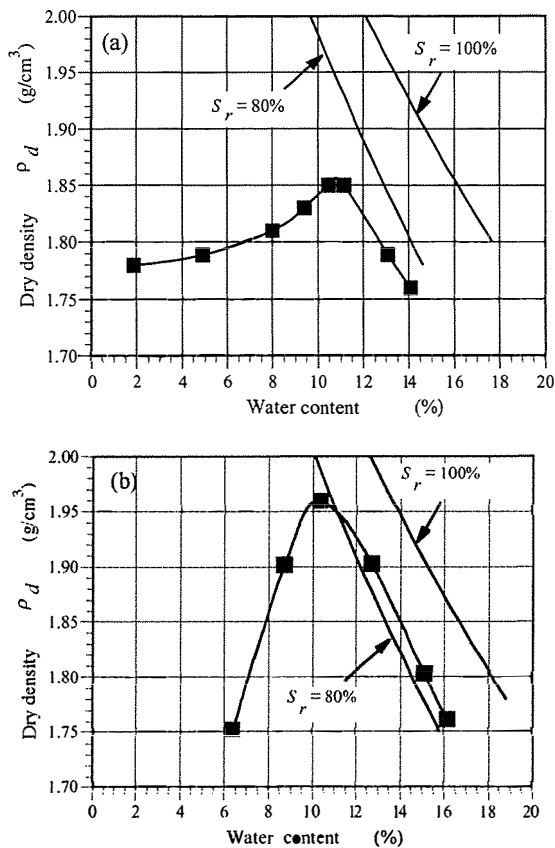


Fig.13. Compaction curves (a) Gray soil, (b) Yellow soil.

2) Experimental test results

(1) In-situ test results

The soil sampling places have already been shown in Fig. 9. A typical soil profile of the sampling sites is shown in Fig. 11. Silt deposits were observed from 10cm below the ground surface to about 30cm depth, followed by sandy soil from 30cm to about 150cm depth and laterite from 150cm to 200cm depth. The changes in the water content from ground surface to 1m depth are shown in Fig. 12. Fig. 12 shows the water content profiles at two points near sampling points ① and ②. Both have peak values at 20-40 cm depth. The peak value at the point near point ① was about 7.5% and that at the point near ② was about 5.6%. The in-situ density tests were also carried out. The results were as follows; for the Gray soil, $\rho_d = 1.57 \text{ g/cm}^3$, $w = 1.3\%$, and for the Yellow soil, $\rho_d = 1.19 \text{ g/cm}^3$, $w = 12.4\%$.

The results of standard compaction tests for the Gray and Yellow soils are shown in Fig. 13. The maximum dry densities (ρ_{dmax}) and optimum water contents (w_{opt}) of both soils were $\rho_{dmax} = 1.855$ and

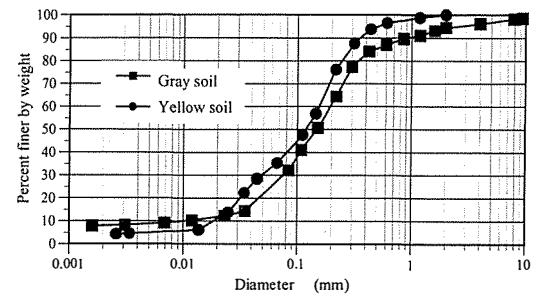


Fig.14. Grading curves for the Gray and Yellow soils.

Table2. Physical properties of Gray and Yellow soils

Properties	Gray soil	Yellow soil
Specific Gravity	2.641	2.672
Sand (%)	67.9	63.9
Slit (%)	27.9	30.5
Clay(%)	4.2	5.6
Maximum Particle Size (mm)	9.5	2.0
Mean Particle Size D_{50} (mm)	0.15	0.11
Uniformity Coefficient	17.2	9.8
Curvature Coefficient	2.4	0.8
Liquid Limit (%)	20	22
Plastic Limit (%)	16	15
Plastic Index	4	7
Soil Type	SM	SM
Field Wet Density (g/cm^3)	1.59	1.34
Field Dry Density (g/cm^3)	1.57	1.19
Natural Water Content (%)	1.3	12.4
Maximum Dry Density (g/cm^3)	1.855	1.960
Optimum Water Content (%)	11.1	10.5

1.960 g/cm^3 and $w_{opt} = 11.1$ and 10.5% , respectively. The maximum dry density was much higher than that obtained from in-situ density test. Yellow soil in the field was very loose.

2) Physical properties of soils

The physical properties of both soils are shown in Table 2. The grading curves are also shown in Fig. 14. In both soils the sand content was higher than 60%. The silt content of the Yellow soil was slightly higher than that of the Gray soil. The maximum particle size of the Yellow soil was 2mm, a lower value than that of the Gray soil, 9.5mm. Both soils may be classified as SM. In the following tests, only the Yellow soil will be used as sample, because silty samples express more remarkable unsaturated behavior like collapse due to wetting.

(3) Volume change behavior

The volume change behavior of the Yellow soil was investigated by using an oedometer and a pressure plate test apparatus. In the oedometer tests, the

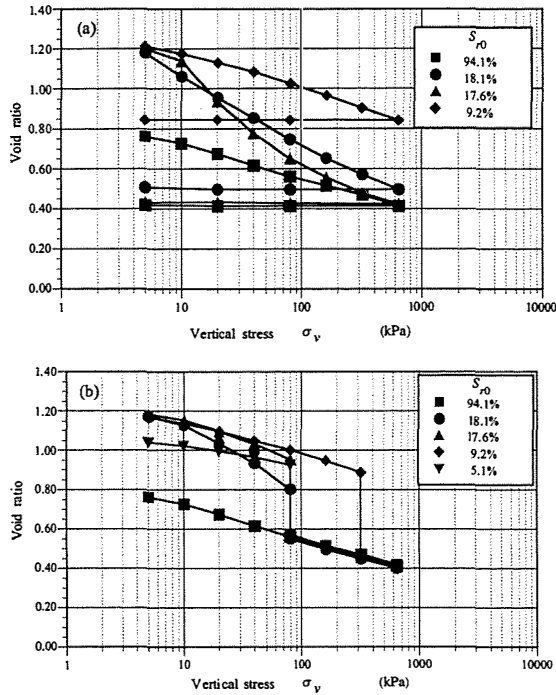


Fig. 15. Relational between void ratio and vertical stress of Yellow soil obtained from aedometer tests. (a) without soaking of water, (b) with soaking of water.

volume change behavior of the specimens with different initial degrees of saturation due to external load was investigated. The pressure plate apparatus was used to study the volume change behavior due to suction.

The results of the oedometer test are shown in Figs. 15, 16 and 17. Fig. 15(a) shows the $e - \log\sigma_v$ relationships without soaking of water. Here, e is the void ratio and σ_v the total vertical stress. Though specimens with high degrees of saturation did not have remarkable yield stresses, the yield stresses increased as the initial degrees of saturation decreased. The suction increases with a decrease in the degree of saturation as seen in Figs. 18 or 19(b). Then, the yield stress increases as the suction increases. It found that the shapes of the $e - \log\sigma_v$ curves could be divided into three groups. The first group corresponded to the $e - \log\sigma_v$ curve for the specimen with the lowest initial degree of saturation, $S_{r0} = 9.2\%$. The yield stress was greater than those of other groups and the slope of the $e - \log\sigma_v$ curve in elastoplastic range was less steep. The second group was the $e - \log\sigma_v$ curve for the almost saturated specimen, $S_{r0} = 94.1\%$. The slope was steeper than that of the first group. The third one corresponded to

the $e - \log\sigma_v$ curves for the specimens with middle range of initial degree of saturation, around $S_{r0} = 18\%$. During the tests, the $e - \log\sigma_v$ curve changed and was close to that under saturated condition. The slopes of the $e - \log\sigma_v$ curves were steeper than those of other groups. All of the $e - \log\sigma_v$ curves at the rebound had the almost same slopes. The influence of the difference in the initial degrees of saturation could not namely be seen in the rebound range.

Fig. 15(b) shows the $e - \log\sigma_v$ relationships with soaking of water. The test results expressed a large amount of volume reductions during soaking of water. The loading paths after soaking of water traced on the saturated loading line. The volume reductions due to soaking of water are called “Collapse due to wetting” and the soil which induces the collapse due to wetting is called a collapsible soil. Thus the Yellow soil is one of collapsible soils.

Fig. 16 shows the coefficient of consolidation $c_v - \sigma_v$ relationship obtained from the saturated sample of

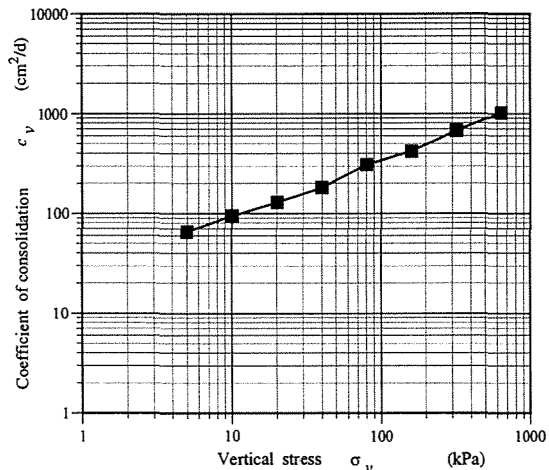


Fig.16. Relationship between coefficient of consolidation and vertical stress of Yellow soil obtained from oedometer tests.

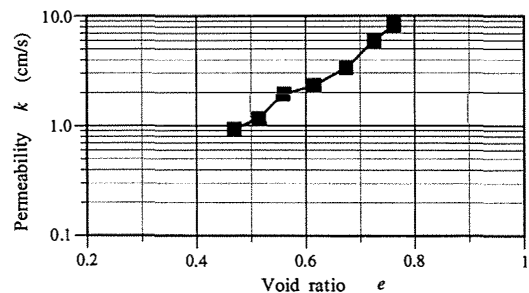


Fig.17. Relationship between permeability and vertical stress of Yellow soil obtained from oedometer tests.

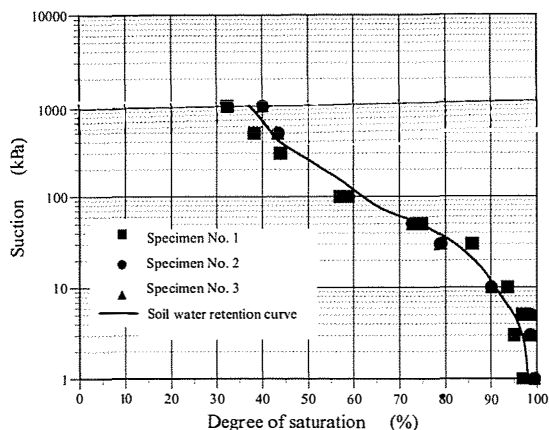


Fig.18. Soil water retention curve for Yellow soil.

the Yellow soil. The values of c_v increased as σ_v increased. The c_v values ranged between 65 and 1000 cm^2/d .

Fig. 17 shows the $k - e$ relationship of the Yellow soil. Here, k is the coefficient of permeability under saturation conditions. The values of k decreased as e decreased. The k values of the Yellow soil ranged between 9×10^{-6} and 8×10^{-5} cm/s .

In the pressure plate test, two series of tests: two tests (No. 1 and 2) for series I and one test (No. 3) for series II, were carried out. The soil-water retention curve for the Yellow soil was obtained from the data of these three tests. The curve is shown in Fig.18. The air entry value was about 10kPa. The suction ranges for three saturation conditions, namely insular air, fuzzy and pendular saturation conditions¹⁰⁾ were approximately $s \leq 10\text{kPa}$, $10\text{kPa} < s < 200\text{kPa}$ and $s \geq 200\text{kPa}$, respectively.

The results of pressure plate test for test No. 3 are shown in Fig. 19. Fig. 19(a) shows the $e - \log s$ relationship. The $e - \log \sigma_v$ relationship of the saturated specimen obtained from oedometer tests is also plotted in this figure. From this figure, the following points can be found. The volume change from points A to B was small. This behavior was elastic. If suction exceeded that at point B, the volume change became larger and the situation continued up to point D. The volume change behavior was elastoplastic. The slope of $e - \log s$ curve was almost the same as that of the $e - \log \sigma_v$ curve in normally consolidated range. This finding indicates that Terzaghi's effective stress equation is

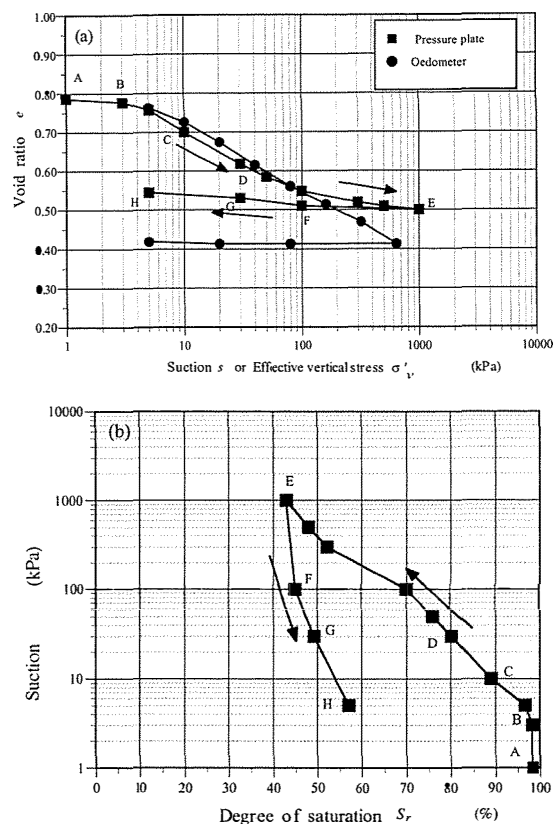


Fig.19. Results of plate tests of Yellow soil (Test No.3).
(a) Relationship between void ratio and suction
(b) Soil-water retention curve.

valid. If the suction value increased over that at point D, the volume change became small again. By reducing suction values from point E to point H through points F and G, the volume increased. The volume change was small. The behavior was elastic. The volume change path from points D to E was almost consistent with that from points E to F. Thus, the behavior from points D to E might also be elastic because the behavior from points E to F was elastic. These features were consistent with those obtained by Fleureau et al⁴⁾.

Fig.19(b) shows the associated soil-water retention curve. Up to point C, the change of the degree of saturation with increasing suction was small. If the suction value exceeded that at point C, air could enter the pores of the soil and the change of degree of saturation became greater. The soil retention curve of the Yellow soil expressed hysteresis due to drying (increasing suction) and wetting (decreasing suction) processes.

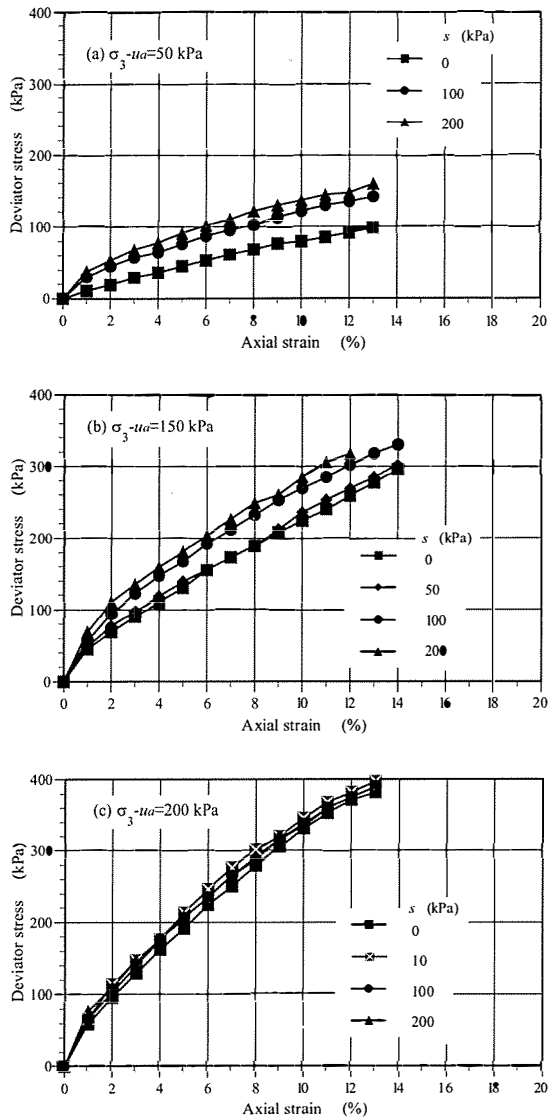


Fig.20. Relationships between deviator stress and axial strain of Yellow soil.

(4) Shear behavior

The conditions of the applied stresses and suction for each specimen are shown in Table 3. The initial conditions are also shown in Table 4. The mean values of the initial void ratio and degree of saturation were 1.22 and 17.7 %, respectively.

Test results are shown in Figs. 20~ 23. Fig. 20 shows the deviator stress q – axial strain ϵ_a curves of specimens with the same confining pressures and different suction values. In all the confining pressures, the higher suction the greater deviator stresses. The shear strength also increased with increasing suction values. However, the difference in the shear behavior due to suction became smaller as the confining pressure increased.

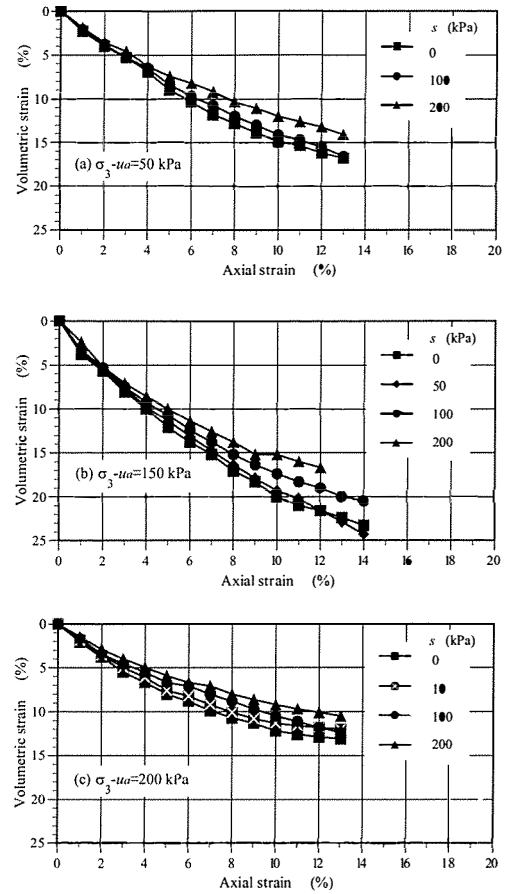


Fig.21. Relationships between volumetric strain and axial strain of Yellow soil.⁵⁾

Table 3. Conditions of stress applied to specimens of the Yellow soil

Specimen No.	Net confining stresses σ_3 (kPa)	Matric suction s (kPa)
T0500	50	0
T0510	50	100
T0520	50	200
T1500	150	0
T1505	150	50
T1510	150	100
T1520	150	200
T2000	200	0
T2001	200	10
T2010	200	100
T2020	200	200

Table 4. Initial conditions of the specimens of Yellow soil

Specimen No.	V_s (cm ³)	W_0 (g)	W (%)	ρ_{d0} (g/cm ³)	e_0	$S_{r,0}$ (%)
T0500	196.35	255.75	7.96	1.206	1.216	17.49
T0510	196.35	255.75	7.98	1.206	1.216	17.54
T0520	196.35	255.75	7.98	1.206	1.216	17.54
T1500	196.35	255.50	8.00	1.205	1.217	17.56
T1505	196.35	256.30	7.95	1.209	1.210	17.56
T1510	196.35	255.59	8.22	1.203	1.221	17.99
T1520	196.35	255.50	8.09	1.204	1.219	17.73
T2000	196.35	256.50	8.00	1.210	1.208	17.70
T2001	196.35	255.50	8.30	1.202	1.223	18.13
T2010	196.35	255.54	7.98	1.205	1.217	17.52
T2020	196.35	255.78	7.98	1.206	1.216	17.54
Average	196.35	255.77	8.04	1.206	1.216	17.67

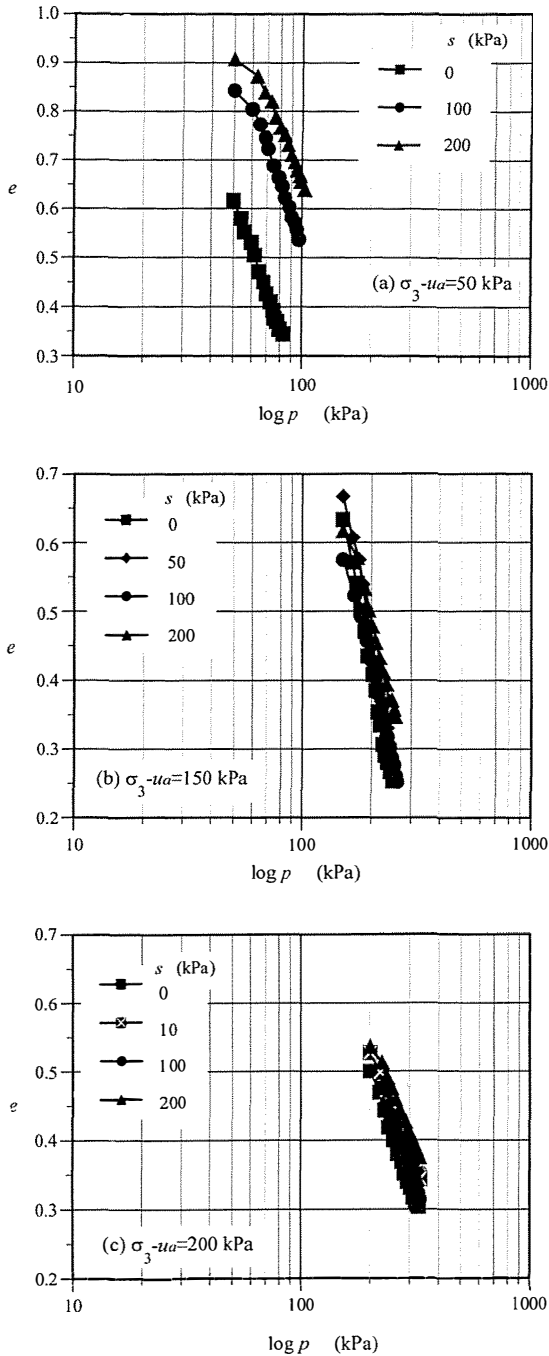


Fig.22. Relationships between void ratio e and mean net stress p of Yellow soil.

Fig. 21 shows the volume change behavior during shear. All the specimens were compressed. Volume change of the specimens with higher suction values was smaller than that of the specimens with lower suction values. Thus, suction inhibited the volume change of the soil.

Fig. 22 shows the $e - \log p$ relationships during shear. Each $e - \log p$ curve consisted of two parts. In the first part, the slopes of $e - \log p$ curves were

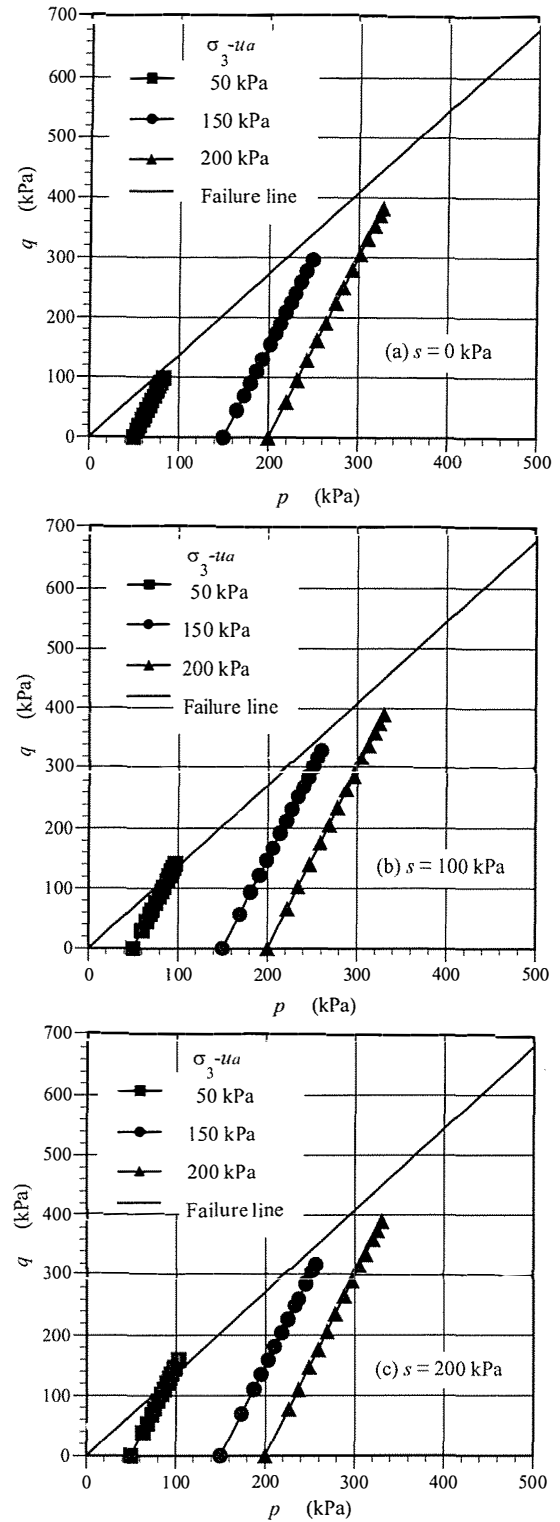


Fig.23. Stress paths of the Yellow soil during shear.

small. In the second part, the slopes of $e - \log p$ curves are much larger than those of the first part. The behavior of the first part was elastic and of the second one elastoplastic. The boundary points between the first and second parts expressed yield points. The yield stresses increased as suction

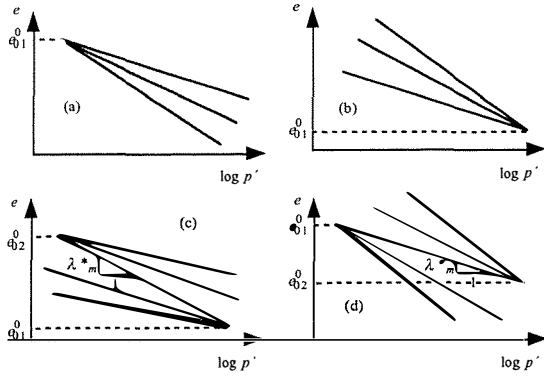


Fig.24. Possible shapes of state surfaces, (a)the slope is monotonically decreasing, (b) the slope monotonically increasing, (c) the slope shows the maximum value, (d)the slope shows the minimum value.

increased. The slopes of the lines in the elastoplastic range became smaller as suction increased.

Fig. 23 shows the stress paths during shear. The failure line was estimated by using the deviator stress values (shear strengths) of specimens with $s = 0\text{kPa}$ at 20 % strain. The shear strength was evaluated by using Kondner's equation¹²⁾. Kondner's equation is as follows;

$$q = \frac{\varepsilon_a}{a+b\varepsilon_a} \quad (7)$$

Where a and b are material parameters. The estimated values of (a, b) for the specimens; T0500, T1500 and T2000 were $(0.0897, 0.0033)$, $(0.0300, 0.0012)$ and $(0.0200, 0.0010)$, respectively. The shear strength parameters were as follows: $\phi' = 33.7^\circ$ ($M = 1.361$) and $c = 0\text{kPa}$.

3) Identification of unsaturated material parameters for yellow soil

We have already proposed elastoplastic models for unsaturated soils^{10), 11)}. In these models, two suction effects were introduced to express the mechanical properties of unsaturated soils. One is that an increase in suction increases effective stresses and the other is that an increase in suction increases yield stress and affects the resistance to plastic deformations. The former effect may be evaluated by the relationship between suction and increases of shear strength due to suction at the critical state. The latter effect may be estimated by formulating the state surface, which expresses the elastoplastic volume change for unsaturated soils.

The effective stress equations are assumed as;

$$\sigma' = \sigma - u_{eq} \quad (8)$$

$$u_{eq} = u_a - s \quad (s \leq s_e) \quad (9)$$

$$u_{eq} = u_a - \left(s_e + \frac{a_e s^*}{s^* + a_e} \right) \quad (s > s_e) \quad (10)$$

Where σ' is the effective stress, σ the total stress, u_{eq} the equivalent pore pressure, a_e a material parameter.

In general, state surfaces may be expressed as;

$$e = -\lambda^* \log p' + \Gamma^* \quad (11)$$

Where λ^* is the slope of $e - \log p'$ line and Γ^* the value of e at $p' = \text{unit}$.

Unsaturated soils may have various shapes of state surfaces. In this paper, we will consider the shapes of state surfaces shown in Fig.24⁸⁾. If the value of λ^* decreases with an increase in suction, the state surface may be expressed as shown in Fig.24(a). Fig.24(b) shows the state surface where the value of λ^* increases oppositely with an increase in suction. Figs. 24 (c) and (d) show the state surfaces where the value of λ^* has maximum or minimum, respectively.

The values of λ^* and Γ^* are assumed to be functions of effective suction s^* . In this paper, the functions are as follows.

When $s^* \leq s_m^*$,

$$\lambda^* = \lambda + \frac{\lambda^*_{f1} s^*}{s^* + a^*_1}, \quad (12)$$

$$\Gamma^* = e_{01}^0 + \frac{\Gamma - e_{01}^0}{\lambda} \lambda^*. \quad (13)$$

When $s^* > s_m^*$,

$$\lambda^* = \lambda^*_{m+} + \frac{\lambda^*_{f2} (s^* - s_m^*)}{(s^* - s_m^*) + a^*_2}, \quad (14)$$

$$\Gamma^* = e_{02}^0 + \frac{\Gamma^*_m - e_{02}^0}{\lambda^*_{m+}} \lambda^*. \quad (15)$$

Where s_m^* is the value of s^* at $\lambda^* = \lambda^*_{m+}$, λ^*_{m+} the maximum or minimum value of λ^* , e_{01}^0 and e_{02}^0 void ratios as shown in Fig. 24, and λ^*_{f1} , λ^*_{f2} , a^*_1 and a^*_2 material parameters.

We will describe a method to estimate the material parameters for effective stresses and the state surface of the Yellow soil, here.

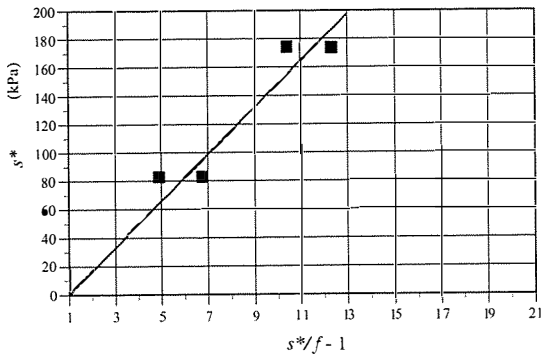


Fig.25. Estimation of effective stress parameters for Yellow soil.

(1) Effective stress parameters

The parameters for effective stresses are estimated as follows.

i) Estimate shear strength for each specimen. The shear strength was assumed to be the values of q for 20 % axial strain. Shear strength was evaluated by using Kondner's equation (Eq. (7)).

ii) Obtain values of $(u_a - u_{eq})$. If the failure always occurs on the failure line, the effective mean stress p' may be obtained from the following equation,

$$p' = \frac{q}{M} \tag{16}$$

The values of $(u_a - u_{eq})$ can be given as

$$(u_a - u_{eq}) = p' - p \tag{17}$$

iii) Identify parameters for effective stresses; s_e and a_e . The air entry value s_e can be evaluated from the soil-water retention curve. Supposing f as;

$$f = u_{eq} - u_a + s_e \tag{18}$$

the relationship between the effective suction s^* and (s^*/f) will become a straight line. Then, the parameter a_e can be estimated as the slope of this line. The s^* - (s^*/f) line for the Yellow soil is shown in Fig.25. The estimated parameters are, $s_e = 10$ kPa and $a_e = 15.2$ kPa. The value of u_{eq} may become a_e when $s^* \rightarrow \infty$.

(2) State surface parameters

The parameters for state surface are estimated as follows.

i) Calculate the effective vertical stresses σ'_v for experimental data obtained from oedometer tests by using the effective stress equations, Eqs. (8) ~ (10).

ii) The associated horizontal stresses σ'_h may be

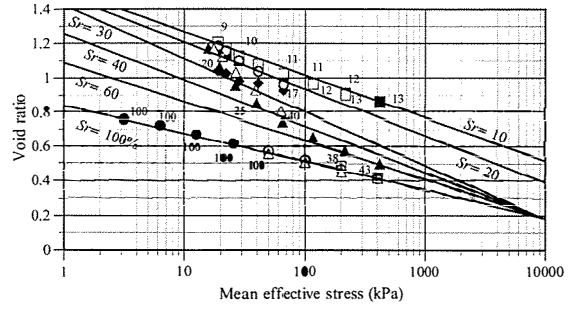


Fig.26. Contour lines of degree of saturation of Yellow soil. (Figures denote the values of degree of saturation).

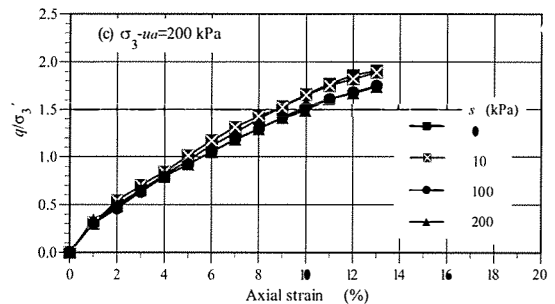
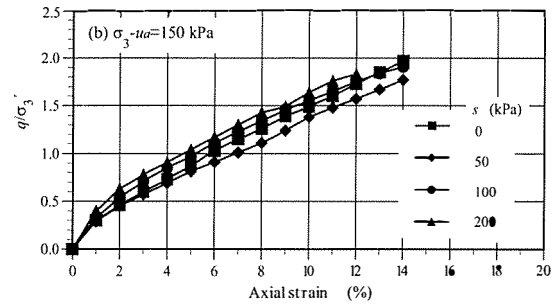
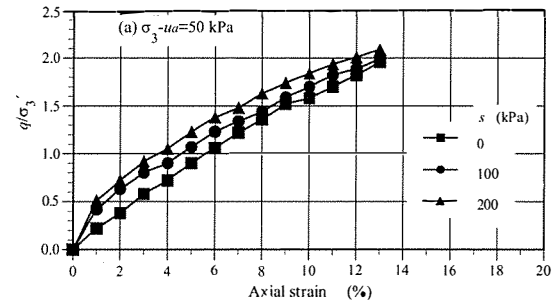


Fig.27. Relationships between normalized deviator stress and axial strain of Yellow soil.

evaluated by Jaky's equation.

$$K_0 = 1 - \sin \phi' \tag{19}$$

$$\sigma'_h = K_0 \sigma'_v \tag{20}$$

iii) Calculate mean effective stress p' as follows.

$$p' = \frac{1}{3} (\sigma'_v + 2\sigma'_h) \tag{21}$$

iv) Plot the experimental data in the $e - \log p'$ space

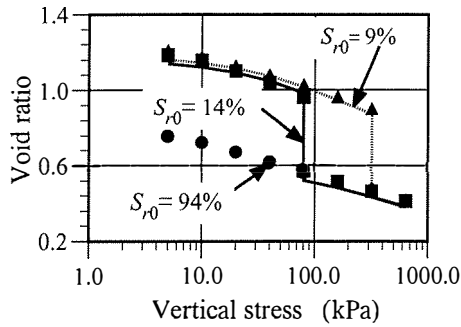


Fig.28. Estimation of effective stress parameters for Yellow soil (Symbols; experimental results, Lines;simulation results).

as shown in Fig. 26.

v) Draw the predicted $e - \log p'$ lines for each degree of saturation S_r in the figure. Here, we selected the degree of saturation $S_r = 10, 20, 30, 40, 60$ and 100% (see Fig.26).

vii) Identify the values of e_{01}^0 and e_{02}^0 , the value λ^*_m and the effective suction s^*_m at $\lambda^* = \lambda^*_m$.

viii) Read the values of the slope λ^* of the $e - \log p'$ lines for $S_r = 10, 20, 30, 40, 60$ and 100% .

ix) Estimate the effective suction values s^* for $S_r = 10, 20, 30, 40, 60$ and 100% from the soil-retention curve.

x) Identify parameters for state surface, λ^*_{f1} and a^*_{1} by using the linear relationship as follows.

$$s^* = \lambda^*_{f1} \left[\frac{s^*}{\lambda^* - \lambda} \right] - a^*_{1} \quad (22)$$

x) Identify parameters for state surface, λ^*_{f2} and a^*_{2} by using the linear relationship as follows.

$$(s^* - s^*_m) = \lambda^*_{f2} \left[\frac{s^* - s^*_m}{\lambda^* - \lambda_m} \right] - a^*_{2} \quad (23)$$

The identified parameters were; $e_{01}^0 = 0.185$, $e_{02}^0 = 1.923$, $s^*_m = 190$ kPa, $\lambda^*_{f1} = 0.244$, $a^*_{1} = 132.0$ kPa. $\lambda^*_{f2} = -0.082$ and $a^*_{2} = 3087.2$ kPa

(3) Plot of experimental results in terms of effective stress expression

Fig. 27 shows the relationships between q/σ'_3 and ϵ_a . The values of σ'_3 were estimated by using identified parameters. The figure shows that the normalized stress-strain curves may be expressed as one curve as the confining pressures increase. Namely, the influence of suction became weaker as

the confining pressures increased. This feature is consistent with those obtained from the test results for unsaturated DL clay and mixed soils⁹⁾.

(4) Verification of identified parameters

In order to verify the state surface parameters, the simulations of oedometer tests on the Yellow soil were carried out by FEM consolidation method⁷⁾.

Fig. 28 shows the simulation results. Simulation results agreed well with the experimental ones. The phenomenon of collapse due to wetting could also be simulated. Thus, the parameters identified were found to be effective.

Conclusions

We investigated the mechanical properties of the Yellow soil which is one of the typical soils distributed in Northeast Thailand. From the results of field density and compaction tests, it found that the soil was depositing very loosely. We also conducted some series of tests for the soil; oedometer, pressure plate and triaxial compression tests. The results of oedometer tests showed that 1) yield stress increased as suction increased, 2) the slopes of $e - \log \sigma'_v$ curves in elastoplastic region were affected by suction, and 3) this soil expressed a large amount of volume reduction during soaking of water namely was a collapsible soil. We also obtained the relationships between the coefficient of consolidation c_v and σ'_v and between the permeability k and void ratio e .

We could identify the air entry value and the suction ranges for three saturation conditions; insular air, fuzzy and pendular saturation conditions from the results of pressure plate tests. The air entry value was about 10kPa. The suction ranges for insular air, fuzzy and pendular saturation conditions were approximately $s \leq 10$ kPa, 10 kPa $< s < 200$ kPa and $s \geq 200$ kPa, respectively. We could also clarify the suction consolidation behavior from the results of pressure plate tests. When the suction value was greater than about 30kPa, the volume change behavior due to suction was elastic.

From the results of triaxial compression tests, the higher suction the greater deviator stress. The shear strength also increased with increasing suction values. However, the difference in the shear behavior

due to suction became smaller as the confining pressure increased. The failure line was estimated by using the deviator stress values (shear strength) of specimens with $s = 0\text{kPa}$ for 20 % strain. The shear strength was evaluated by using Kondner's model. We obtained the shear strength parameters $\phi' = 33.7^\circ$ ($M = 1.361$) and $c = 0\text{kPa}$.

The identification of unsaturated material parameters of the Yellow soil for the elastoplastic model was conducted by using data of oedometer, pressure plate and triaxial compression tests. The parameters related to effective stress were as follows; $s_e = 10\text{kPa}$ and $a_e = 15.2\text{kPa}$. The parameters for state surface were as follows; $e_{01}^0 = 0.185$, $e_{02}^0 = 1.923$, $s_m^* = 190\text{kPa}$, $\lambda_{f1}^* = 0.244$, $a_1^* = 132.0\text{kPa}$, $\lambda_{f2}^* = -0.082$ and $a_2^* = 3087.2\text{kPa}$.

Acknowledgments

We would like to express our sincere gratitude to Prof. Kenji Ishihara, Dr. Mitsutaka Sugimoto, Dr. Satoru Shibuya, Prof. A. S. Balasubramaniam, Prof. D. T. Bergado, Prof. Prinya Nutalaya, Dr. Keiji Kainuma, Dr. Koji Kawashima and Dr. M. Imaizumi for their advice and contributions. We also thank the associated scientists, faculties and staffs of AIT and JIRCAS. This work was performed under the collaborative research project between AIT and JIRCAS.

References

- 1) Boonsaner, M. (1977). Engineering geology of the town of Khon Kaen, Northeastern Thailand. Master Thesis, Asian Institute of Technology (AIT), 1-120.
- 2) Chong, K. Y. (1988). Geohydrology of the town of Khon Kaen, Northeastern Thailand. Master Thesis, Asian Institute of Technology (AIT), 1-115.
- 3) Department of Mineral Resources (1987). Geological map of Thailand Scale 1:2,500,000.
- 4) Fleureau, J. M., Saoud, S. K., Soemitro, R. and Taibi, S. (1993). Behavior of clayey soils on drying-wetting paths, *Can. Geotech. J.* 30, 287-296.
- 5) Fredlund, D. G. and Rahardjo, H (1993). Soil mechanics for unsaturated soils, John Wiley & Sons Inc., 1-517.
- 6) JGS (1990). Methods and explanations of soil testing, Japanese Geotechnical Society (JGS), 289-315 (in Japanese).
- 7) Kohgo, Y. (1997). Method of analysis of saturation collapse behavior, *JIRCAS J.*, No. 4, 1-28.
- 8) Kohgo, Y. (1999). State surface and its modelling, *Proc. of 34th Japan Natl. Conf. on Geotechnical Eng.*, The Japanese Geotechnical Society, Vol. 1, 757-758 (in Japanese).
- 9) Kohgo, Y. and Moriyama, H. (1998). Volume change and shear behavior of unsaturated silt and sand/clay mixed soil under triaxial stress conditions, *Trans. of JSIDRE No. 193*, 35-49 (in Japanese with English summary).
- 10) Kohgo, Y., Nakano, M. and Miyazaki, T. (1993). Theoretical aspects of constitutive modelling for unsaturated soils. *Soils and Foundations Vol. 33*, No. 4, 49-63.
- 11) Kohgo, Y., Nakano, M. and Miyazaki, T. (1993). Verification of the generalized elastoplastic model for unsaturated soils. *Soils and Foundations Vol. 33*, No. 4, 64-73.
- 12) Kondner, R. L. (1963). Hyperbolic stress-strain response cohesive soils, *Proc. ASCE* 89, No. SM1, 115-143.
- 13) Kono, Y., Sopaphun, P. and Nakamura, Y. (1997). Transformation of agricultural development in Thailand. *J. JSIDRE* 65, No. 4, 383-389 (in Japanese).
- 14) Udomchoke, V. (1991). Origin and engineering characteristics of the problem soils in the Kohrat Basin, Northeastern Thailand. Doctor Thesis, Asian Institute of Technology (AIT), 1-415.
- 15) Yamasaki, K. (1997). Guidance of the Royal Irrigation Department and activities of JICA specialists, *The 115th Proc. of Agricultural Engineering in Thailand*, 29-34 (in Japanese).

東北タイに分布する典型的な土の飽和・不飽和力学的特性

向後 雄二^{a)}, スレンドラ バハデュル タムラカル^{b)}, フイ ガン タン^{b)}

^{a)} 国際農林水産業研究センター生産利用部
(〒 305-8686 茨城県つくば市大わし 1-2)

^{b)} アジア工科大学院大学
(〒 12120 タイ国パトタニ県クルンルアング)

摘要

東北タイに分布する典型的な土の飽和および不飽和状態での力学的特性を調べた。典型的な土として黄色土 (Yellow soil) をサンプリングし、この土の特性を圧密試験機、加圧板試験機および三軸圧縮試験機を用いて調べた。圧密試験の結果より、サクシヨンの増加とともに降伏応力が増加すること、弾塑性領域での間隙比 - 鉛直応力 (対数表示) 曲線の傾きはサクシヨンによって大きな影響を受けること、およびこの土は水浸によって大きな圧縮変形を生じることがわかった。加圧板試験の結果より、この土の空気侵入値は約 10kPa であること、およびサクシヨンの値が 30kPa を超えるサクシヨンに対しては弾力的な体積変化挙動を示すこ

とがわかった。三軸圧縮試験の結果より、全ての拘束圧で、同じ軸ひずみでの偏差応力を比較すると、高いサクシヨンを作用させた供試体の偏差応力の方が小さなサクシヨンを作用させた供試体のそれより大きいこと、せん断強度もサクシヨンの増加とともに大きくなること、しかし、そのサクシヨンによる影響は拘束圧の増加とともに小さくなること、がわかった。これらの試験結果より、筆者らが提案している不飽和土を対象とした弾塑性モデルのパラメータの同定を、その方法とともに詳述した。また、同定したパラメータの適用性についても簡単に検討した。

キーワード：コラップス土、砂質土、サクシヨン、不飽和土